Ξ^- Production by Σ^-,π^- and Neutrons in the Hyperon Beam Experiment WA89 * at CERN

M. HEIDRICH[a], representing the WA89–Collaboration

[a]Max Plank Institut für Kernphysik Heidelberg, Germany

We report on the measurement of the cross sections of Ξ^-–hyperons produced in high energy Σ^-–, π^-– and neutron–interactions in copper and carbon. Measuring the p_t–, x_f– and A–dependence of the production cross sections for the different projectiles, we observed a strong leading particle effect for Ξ^- produced by Σ^-. This constitutes the first measurement using three different projectiles and two different targets within the same experiment ensuring small systematic uncertanties.

1. Introduction

The inclusive production of Ξ^-–Hyperons in high energy collisions of different hadrons with target nuclei allows to study the role of the projectile valence quarks in the production process. It gives therefore insight in the physics of the hadronisation process.
The inclusive production of hyperons has been studied mostly in proton– and neutron–beams [1][7]. Ξ^-–production in Ξ^-–Be– and Ξ^-–N–interactions was measured in a previous experiment with the SPS charged hyperon beam at CERN [11,12]. The measurements were performed in different kinematical regions and therefore a comparison of the different results is difficult.
The WA89 experiment gives the opportunity to measure the Ξ^-–production under homogeneous conditions with different types of beam particles on several targets.

2. Experiment WA89

The Experiment WA89 (Fig. 1) was performed using the charged hyperon beam of the CERN SPS. Its main purpose is to study the production of charmed baryons and to search for exotic states. The production studies of Ξ^- were performed in parallel with the main program.

*supported by the Bundesministerium für Forschung und Technologie, Germany, under contract numbers 05 5HD15I, 06 HD524I and 06 MZ5265

Hyperons were produced by 450 GeV/c protons impinging on a beryllium target. A subsequent magnetic channel selected negative particles with a momentum of 345 GeV/c and a momentum spread of $\sigma(p)/p = 9\%$. After a distance of 16 m this secondary beam hit the experimental target which consisted of one copper and three carbon blocks. The copper target had a thickness corresponding to 2.6 % of an interaction length. The thickness of each carbon block corresponded to 0.83 % of an interaction length. The size of the beam at the experimental target was 3.6 cm horizontally and 1.5 cm vertically. An average beam spill of 2.1 s contained about $1.8 \cdot 10^5$ Σ^-–hyperons and about $4.5 \cdot 10^5$ π^- at the experimental target for an incoming intensity of $3.0 \cdot 10^{10}$ protons per spill.
A transition radiation detector (TRD) was used to discriminate online between π^- and hyperons. In special runs π^-– interactions were recorded for normalisation purposes.
The beam and the secondary particles were detected by silicon microstrip–planes with 25 and 50μm pitch. Positioning the target about 14 m upstream of the centre of the Ω-spectrometer provided a 10 m long decay area for short living strange particles. The products of these decays along with the particles coming directly from the target were detected by drift chambers. Special MWPC chambers were used in the central region of high particle fluxes. The particle momenta were measured by the Ω-spectrometer [14] con-

sisting of a super-conducting magnet with a field integral of 7.5 Tm and a tracking detector consisting of MWPCs and drift chambers. Further downstream a Ring Imaging Cherenkov Detector (RICH) [15], a Lead Glass Calorimeter [16] and a Hadronic Calorimeter allowed for particle identification but were not used in this analysis.
We present here results of the analysis of about 100 million events recorded in 1993.

3. Event Reconstruction

Ξ^- were reconstructed in the decay chain $\Xi^- \rightarrow \Lambda^0\pi^- \rightarrow p\pi^-\pi^-$. In the search for $\Lambda^0 \rightarrow p\pi^-$ decays criteria on the decay vertex were applied. To select candidates for the Ξ^-–decay, the invariant mass of the reconstructed Λ^0 was required to be within a mass window of 3σ ($\sigma \approx 3.7$ MeV/c^2) around the reference mass. The Ξ^- trajectory had to be measured in the vertex detector and we cut on the parameters of the Ξ^-–decay vertex.
To identify Σ^- and π^- interactions we required the transverse distance of the Σ^-– or π^-–beam track to the reconstructed vertex position to be less than 6σ, ($\sigma \approx 25\mu m$) and the beam track not to be connected to any outgoing track.
To identify interactions of neutrons stemming from Σ^-–decays upstream the experimental target, the following criteria were imposed: No high momentum π^- was detected in the TRD (π^- from Σ^-–decays are below the TRD threshold), the π^-–track from the Σ^-–decay missed the reconstructed interaction point by at least 6σ and the π^-–track was connected to a track in the spectrometer.

4. Beam conditions

The negative beam particles (Σ^- , π^-) had an average momentum of 345 GeV/c and a momentum spread of $\sigma(p)/p = 9\%$. Since the beam momentum in each individual event was not measured we used the average momentum of 345 GeV/c for the analysis. The momentum of the neutron was defined as the difference between the average Σ^-–momentum and the π^-–momentum measured in the spectrometer. The neutron spectrum has an average momentum of 260 GeV/c and a width of $\sigma(p)/p = 15\%$.
Despite the beam particle identification in the TRD the Σ^-– respectively π^-–beam was contaminated by misidentified π^-, Σ^-, $\Xi^-$and neutrons. Therefore, the beam composition for each data set was studied in a dedicated analysis.
To measure the Ξ^-–contamination of the Σ^--beam a sample of events with beam particles passing through the target without interaction was used. In this data sample we identified Σ^-– and Ξ^-–decays by the correlation between the decay angle (angle between the incoming beam particle and the daughter–π^- in the decays $\Xi^- \rightarrow \Lambda\pi^-$ or $\Sigma^- \rightarrow n\pi^-$) and the momentum of the daughter–π^- measured in the spectrometer. With this method we obtain a Ξ^- to Σ^- ratio of $(1.2 \pm 0.1)\%$. This contribution was subtracted from the differential cross sections taking the $\Xi^- + A \rightarrow \Xi^- + X$ cross section from [11].
Further contamination of the Σ^-–beam comes from misidentified π^- . The π^- to Σ^- ratio was measured offline evaluating the pulse height information of each TRD chamber. We obtained a value of $(12.5 \pm 2.5)\%$.
In addition the Σ^- data sample was contaminated by low momentum π^- stemming from Σ^-–decays upstream of the experimental target. This π^- to Σ^- ratio was determined in a Monte Carlo simulation to amount to 28 % . Beam Σ^- show a strong correlation between their incident angle and their position at the experimental target. A cut on this correlation not being fullfilled by π^- from Σ^-–decays allows to suppress this background.
The π^-–sample was contaminated by misidentified Σ^- . Analysing the TRD pulseheight information, we measured the remaining Σ^-–contamination in the pion data sample to be $1 \pm 1.5\%$.
The sample of neutron interactions was contaminated by Λ^0–interactions stemming from Ξ^---decays upstream of the experimental target. From the measured Ξ^- to Σ^-ratio one yields a Λ^0 to neutron ratio of $(1.2 \pm 0.1)\%$. We assume the production cross section for Ξ^- by Λ^0 to be as large as the one by Σ^- and correct for this background.

5. Detector Efficiencies and Systematics

The large aperture of the spectrometer provided a relatively flat apparatus function in the whole region of the kinematic variables x_F and p_T . To measure the reconstruction efficiency we generated Ξ^- assuming a uniform x_F distribution for $0 < x_F < 1$ and a p_t^2 dependence of the form $d\sigma/dp_t^2 \sim exp(-3p_t^2)$. A complete detector simulation was performed in the frame of GEANT 3.15 [20]. The simulated events were subsequently passed through the event reconstruction chain.
The uncertainty in the efficiency is an important source of systematic error in the measurements. To estimate this uncertainty we varied the event selection criteria applied to the data and the simulated events. The resultant changes in the obtained cross sections are of the order of 10 %.
A larger systematic uncertainty comes from the normalisation of our measured cross sections. We estimate this error to be as high as 30%.

6. Results

The differential cross sections as function of x_F are shown in Fig. 2. We observe a strong leading particle effect for Ξ^-–production by Σ^- . Fig. 3 shows the differential cross sections as function of p_t^2. A systematic deviation from the exponential behaviour is visible at high values of p_t^2. The following parametrisation was used for the approximation of our data:

$$\frac{d^2\sigma}{dp_t^2 dx_F} = C(1-x_F)^n exp(-bp_t^2)$$

where the three parameters C,b and n were assumed to be independent of p_t^2 and x_F. The error bars contain the statistical error contribution from data and Monte Carlo.
To obtain a total cross section we integrated the measured differential cross sections. For the neutron and π^- the data were extrapolated from the measured range $0 < x_F < 0.6$ to the total range with the parameters obtained in the fits to the differential cross section.
The ratio of the cross sections for the copper and carbon targets for the different incident particles can be directly translated into a dependence on the atomic number A of the target material. We used the conventional parametrisation

$$\sigma = \sigma_0 \cdot A^\alpha .$$

The ratio of the differential cross sections allows us to demonstrate the variation of the parameter α versus x_F and p_t^2 (Fig. 4).

7. Discussion and conclusion

In fig. 5 a) we present our result on the Ξ^- production cross section in neutron–induced reactions together with data for proton–induced reactions at similar energies. Our result agrees well with the existing proton data.
The cross sections for pion–induced Ξ^-–production, however, is about a factor 10 higher than existing data as shown in fig. 5 b). In contrast to the old measurement our data on Ξ^-–production by pions is only about 30% smaller than the corresponding value for protons (fig. 5 a)). This is in good agreement with the ratio of the total inelastic cross sections for $\pi^-$and protons.
In fig. 6 a) and b) we compare our data on Ξ^-–production by Σ^- with other production cross sections of hyperons by different projectiles. Figure 6 a) shows the x_F–dependence of Ξ^-–production by protons, Σ^- and Ξ^- . Although projectile and produced Ξ^- differ in strangeness by different amounts the three cross sections are equal at small x_F. At large x_F a leading effect is observed for Ξ^-– and Σ^-–projectiles, which is strongest for Ξ^- but clearly visible also for Σ^- .
In fig 6 b) we compare three reactions in which projectile and produced particle differ by one unit of strangeness. Here the cross sections are of approximately equal size at large x_F , but differ by about one order of magnitude at small x_F.
The two figures both indicate that in the central region all strange quarks of the final state are produced in the interaction process. In the projectile fragmentation region, however, the cross sections depend strongly on the overlap of the strange quark content of projectile and produced particle. This is an interesting observation, since no such dependence on the overlap of light quarks between initial and final state exists (fig. 5 a)).

8. Acknowledgements

We are indebted to J.Zimmer and the late Z.Kenesei for their help during all moments of detector construction and set-up. We are grateful to the staff of CERN's EBS group for providing an excellent hyperon beam channel, to the staff of CERN's Omega group for their help in running the Ω–spectrometer and also to the staff of the SPS for providing good beam conditions.

REFERENCES

1. J.Badier et al., Phys. Lett. **B39**, 414 (1972)
2. V.Hungerbühler et al., Phys.Rev. **D12**, 1203 (1975)
3. M.Bourquin et al., Nucl. Phys. **B153**,13 (1979)
4. S.Erhan et al., Phys. Lett. **B85**, 447 (1979)
5. M.Baubillier et al., Nucl. Phys. **B192**,1-17 (1981)
6. M.Bourquin et al., CERN-EP/80-25,1980
7. T.R.Cardello et al., Phys.Rev. **D32**, 1 (1985)
8. A.N.Aleev et al., Yad. Fiz. **44**, 661 (1986)
9. H.C.Fenker et al., Phys.Rev. **D30**, 872 (1984)
10. S.Mikocki et al., Phys.Rev. **D34**, 43 (1986)
11. S.F.Biagi et al., Z.Phys.C Particles and Fields 9, 305 (1981)
12. S.F.Biagi et al., Z.Phys.C Particles and Fields 34,187 (1987)
13. P.Skubic et al., Phys.Rev. **D18**, 3115 (1978)
14. W.Beusch, CERN–SPSC/77-70, CERN, Geneva, Switzerland (1977)
15. W. Beusch et al., Nucl. Instrum. Methods **A323**, 373 (1992)
16. W.Brückner et al., Nucl. Instrum. Methods **A313**, 345 (1992)
17. Particle Data Group; K.Hikasa et al., Phys. Rev. **D45**(1992) 39, 499 (1988)
18. R.E.Ansorge et al., Nucl.Phys. **B103**, 509 (1976)
19. B. Andersson et al., Z.Phys. **C57**, 485-494 (1993) H.Pi,Comput. Phys. Commun. **71**,173-192 (1992)
20. GEANT 3.21 CERN Program Library W5103, CERN 1993

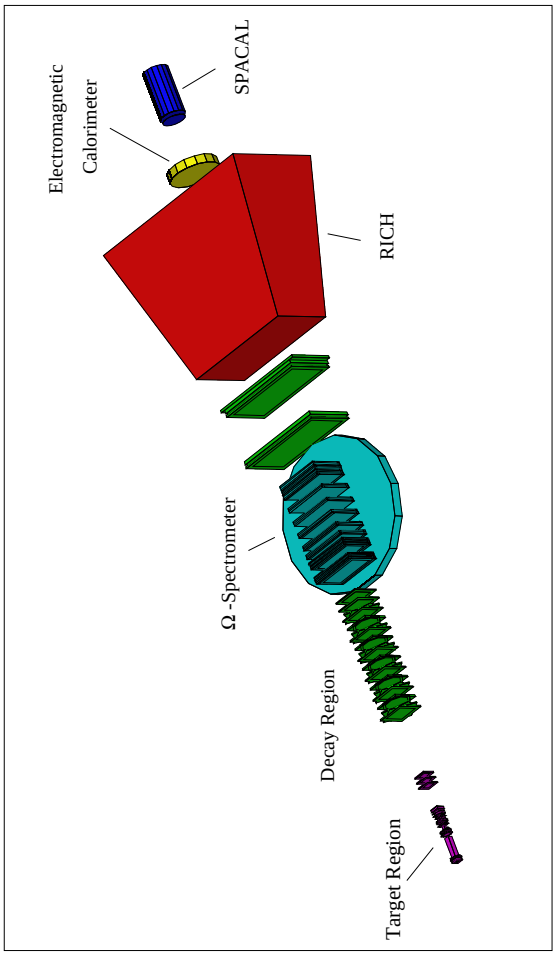

Figure 1. Setup of the WA89 experiment in the 1993 run

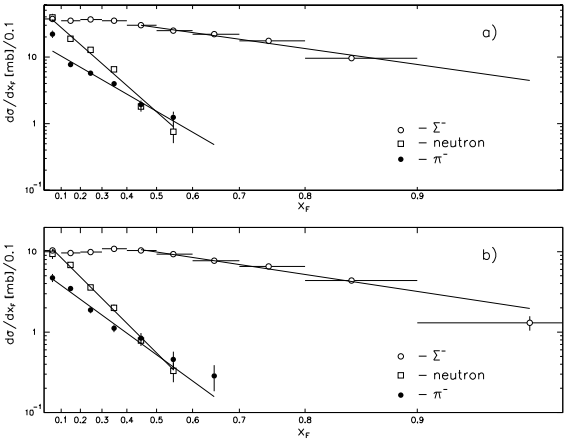

Figure 2. The differential cross section $d\sigma/dx_F$ as function of x_F integrated over p_t^2 in case of neutron–,π^-– and Σ^-–interactions in a) copper, b) carbon.

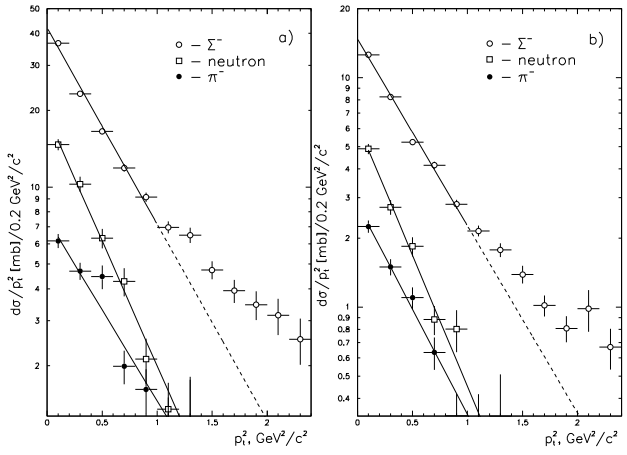

Figure 3. The differential cross section $d\sigma/dp_t^2$ as function of p_t^2 integrated over x_F in case of neutron–,π^-– and Σ^-–interactions in a) copper, b) carbon.

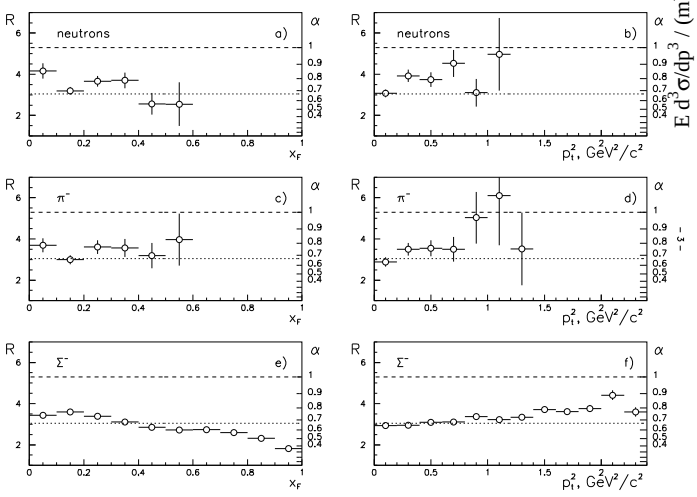

Figure 4. The A–dependence of the Ξ^-–cross section as function of x_F and p_t^2 for (a-b) neutron–; (c-d) π^-– and (f-g) Σ^-–interactions. R=$\sigma_{Cu}/\sigma_C \cdot A_C/A_{Cu}$; $\sigma \propto A^\alpha$

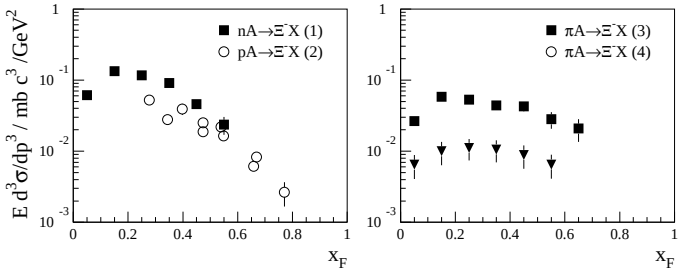

Figure 5. Ξ^-–production cross sections at $p_t^2 < 0.2\ GeV^2/c^2$ (a) (1) $nA \to \Xi^- X$ at 345 GeV/c this measurement (2) $pA \to \Xi^- X$ at 200 GeV/c and [3,7], (b) (3) $\pi A \to \Xi^- X$ at 345 GeV/c this measurement, (4) $\pi A \to \Xi^- X$ at 200 GeV/c [10].

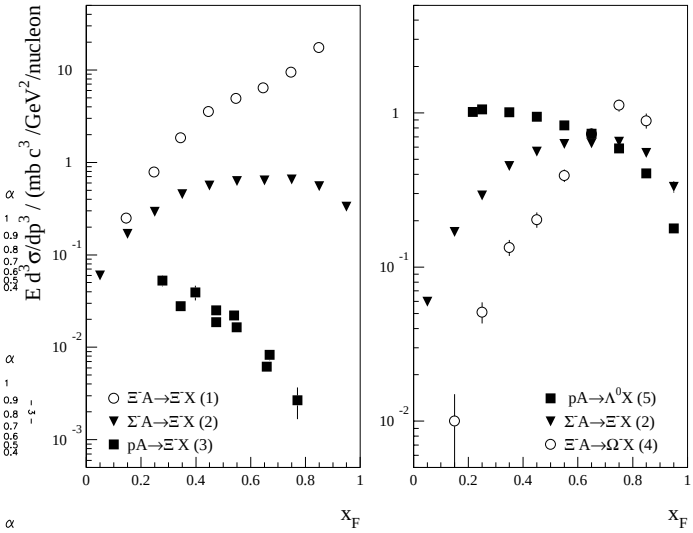

Figure 6. Invariant production cross sections at $p_t^2 < 0.2\ GeV^2/c^2$ in reactions with (a) $\Delta S = 0$ $\Delta S = 1$ and $\Delta S = 2$ between projectile and final state Ξ^- . (b) $\Delta S = 1$ between projectiles and final state particle. References: (1) $\Xi^- A \to \Xi^- X$ at 116 GeV/c [12], (2) $\Sigma^- A \to \Xi^- X$ at 345 GeV/c this measurement, (3) $pA \to \Xi^- X$ at 200 GeV/c and at 400 GeV/c [3,7], (4) $pA \to \Lambda^0 X$ at 300 GeV/c [13], (5) $\Xi^- A \to \Omega^- X$ at 116 GeV/c [12].